

Lattice Boltzmann model for liquid-vapour thermal flows

Sergiu Busuioc^{a,b,*}, Victor E. Ambrus^{a,b}, Tonino Biciuşcă^{a,b}, Victor Sofonea^a

^aCenter for Fundamental and Advanced Technical Research, Romanian Academy
Bd. Mihai Viteazul 24, 300223 Timișoara, Romania

^bDepartment of Physics, West University of Timișoara, Bd. Vasile Pârvan 4, 300223 Timișoara, Romania

Abstract

We developed a two-dimensional Lattice Boltzmann model for liquid-vapour systems with variable temperature. Our model is based on a single particle distribution function expanded with respect to the full-range Hermite polynomials. In order to ensure the recovery of the hydrodynamic equations for thermal flows, we used a fourth order expansion together with a set of momentum vectors with 25 elements whose Cartesian projections are the roots of the Hermite polynomial of order $Q=5$. Since these vectors are *off-lattice*, a projection scheme involving flux limiters is used to evolve the corresponding set of distribution functions. A third order scheme employing a 25 point stencil is used to compute the gradient operators in the force term that ensures the liquid-vapour phase separation and diffuse reflection boundary conditions are used on the walls. We investigated the liquid-vapour phase separation between two parallel walls kept at a constant temperature T_w smaller than the critical temperature T_c . The effect of the spurious velocity on the temperature profile was found to be smaller than 1.0%, even when $T_w < 0.7 T_c$.

Keywords: Lattice Boltzmann, Gauss-Hermite quadrature, off-lattice, liquid-vapor phase separation

1. Introduction

Lattice Boltzmann (LB) models with variable temperature are known since at least two decades [1, 2, 3] and their development is still in progress today. Basically, the thermal LB models belong to one of the following families [4, 5]: *multi-speed models* [6, 7, 8, 9, 10, 11, 12, 13, 14, 15], *double distribution function models* [16, 17, 18, 19, 20, 21] and hybrid models [22, 23, 24, 25, 26, 27, 28, 29]. Such models are currently applied to investigate physical and engineering processes involving heat transfer with or without phase change, as well as micro- and nano-scale flow phenomena. The diversity of these applications are confirmed by the rich literature related to LB models and by two series of regular conferences [30, 31].

At time t , the non-dimensionalized [9, 12] local values of the fluid particle number density $n \equiv n(\mathbf{x}, t)$, velocity $\mathbf{u} \equiv \mathbf{u}(\mathbf{x}, t)$ and temperature $T \equiv T(\mathbf{x}, t)$ can be retrieved through the calculation of the moments (up to second order) of the single particle distribution function $f \equiv f(\mathbf{x}, \mathbf{p}, t)$ defined in the point (\mathbf{x}, \mathbf{p}) of the phase space [4, 11, 32]. Current multispeed LB use the Cartesian coordinate system in the D -dimensional momentum space and the moments of $f(\mathbf{x}, \mathbf{p}, t)$ are computed using a convenient quadrature. For this purpose, $f(\mathbf{x}, \mathbf{p}, t)$ is approximated by its expansion $f^N(\mathbf{x}, \mathbf{p}, t)$ up to a certain order N with respect to a set of orthogonal polynomials, e.g., the full-range Hermite polynomials defined on each Cartesian axis of the momentum space [4, 11, 32, 33, 34, 35]. The resulting quadrature points $\{\mathbf{p}_\kappa \equiv (p_{k_1}, p_{k_2}, \dots, p_{k_D})\}$ form a discrete vector set in the momentum space ($\kappa \equiv k_1 k_2 \dots k_D$ is a set of integer indices and p_{k_α} , $1 \leq \alpha \leq D$ are the projections of the vector \mathbf{p}_κ on the Cartesian axes). As a result of the application of the Gauss-Hermite quadrature method, in the LB model the fluid system is described by the set of functions $f_\kappa \equiv f_\kappa(\mathbf{x}, t) = f^N(\mathbf{x}, \mathbf{p}_\kappa, t)$, defined in the nodes \mathbf{x} of a lattice \mathcal{L} .

*Corresponding author

Email addresses: sergiu.busuioc@e-uvt.ro (Sergiu Busuioc), victor.ambrus@e-uvt.ro (Victor E. Ambrus), biciusca.tonino@gmail.com (Tonino Biciuşcă), sofonea@acad-tim.tm.edu.ro (Victor Sofonea)

In the D -dimensional LB model where the full-range Gauss-Hermite quadrature of order Q is used on each Cartesian axis, we have $1 \leq k_\alpha \leq Q$ for all α , $1 \leq \alpha \leq D$, and hence the momentum set $\{\mathbf{p}_\kappa\}$ has $K = Q^D$ elements. The order Q of the quadrature should satisfy the condition $Q \geq N + 1$ in order to retrieve *all* the moments of $f(\mathbf{x}, \mathbf{p}, t)$ up to order N [11, 33, 34, 36]. Although the number K of the quadrature points can be reduced by very elaborated pruning techniques by sacrificing some higher order moments of the distribution function [11, 37, 38],

we will not consider such models in this paper. For thermal problems, the moments of the distribution function $f(\mathbf{x}, \mathbf{p}, t)$ up to order $N = 4$ are needed in order to get the evolution equations of the macroscopic fields at the Navier - Stokes - Fourier level [4, 7, 11, 39]. Thus, the minimum number of the momentum vectors in the two-dimensional ($2D$) thermal LB model based on the full-range Gauss-Hermite quadrature that ensures all the moments of $f(\mathbf{x}, \mathbf{p}, t)$ up to order $N = 4$ is $K = (N + 1)^2 = 25$. The purpose of this paper is to explore the capabilities of this minimal model when simulating the behaviour of a phase-separating fluid that obeys the Van der Waals equation of state.

2. Description of the model

2.1. Evolution equation and the equilibrium functions f_κ^{eq}

Let us consider the two-dimensional ($D = 2$) lattice Boltzmann model of order $N = 4$, where the full-range Gauss-Hermite quadrature of order $Q = 5$ is used on each Cartesian axis. The quadrature points in the two-dimensional momentum space, namely, $\mathbf{p}_\kappa \equiv (p_{k_1}, p_{k_2})$, $1 \leq k_1, k_2 \leq Q$, are constructed using a direct product rule [11, 34, 35]. In this case, $p_{k_\alpha} \in \{\mathcal{R}_q\}$ for all $\alpha \in \{1, 2\}$, where \mathcal{R}_q , $1 \leq q \leq Q$ are the roots of the full-range Hermite polynomial of order Q [11, 40, 34]. For convenience, Table 1 shows the roots of the full-range Hermite polynomial $H_5(p)$, as well as their associated weights \mathcal{W}_q given by [41, 42, 43, 34, 35]

$$\mathcal{W}_q = \frac{Q!}{[H_{Q+1}(\mathcal{R}_q)]^2}. \quad (1)$$

To avoid confusion, we recall that the full range Hermite polynomials $H_\ell(p)$ used in this paper are the so-called *probabilistic* Hermite polynomials, which are orthogonal with respect to the weight function

$$\omega(p) = \frac{1}{\sqrt{2\pi}} e^{-p^2/2}, \quad (2)$$

and their orthogonality relation reads [41]

$$\int_{-\infty}^{+\infty} dp \omega(p) H_\ell(p) H_{\ell'}(p) = \ell! \delta_{\ell, \ell'}. \quad (3)$$

Table 1: The roots \mathcal{R}_q of the full-range Hermite polynomial of order $Q = 5$ and their associated weights \mathcal{W}_q [11].

q	\mathcal{R}_q	\mathcal{W}_q
1	$-\sqrt{5 + \sqrt{10}}$	$(7 - 2\sqrt{10})/60$
2	$-\sqrt{5 - \sqrt{10}}$	$(7 + 2\sqrt{10})/60$
3	0	8/15
4	$\sqrt{5 - \sqrt{10}}$	$(7 + 2\sqrt{10})/60$
5	$\sqrt{5 + \sqrt{10}}$	$(7 - 2\sqrt{10})/60$

As usual in the current LB models involving the BGK collision term [11], the non-dimensionalized form of the evolution equation of the functions $f_{\boldsymbol{\kappa}}$ for a single-component fluid is:

$$\partial_t f_{\boldsymbol{\kappa}} + \frac{1}{m} \mathbf{p}_{\boldsymbol{\kappa}} \cdot \nabla f_{\boldsymbol{\kappa}} + \mathbf{F} \cdot (\nabla_{\mathbf{p}} f)_{\boldsymbol{\kappa}} = -\frac{1}{\tau} [f_{\boldsymbol{\kappa}} - f_{\boldsymbol{\kappa}}^{eq}], \quad (4)$$

where \mathbf{F} is the force acting on a particle of mass $m = 1$ and τ is the relaxation time. The Cartesian components $(\partial_{p_\alpha} f)_{\boldsymbol{\kappa}}$, $\alpha \in \{1, 2\}$ of the elements in the discrete vector set $\{(\nabla_{\mathbf{p}} f)_{\boldsymbol{\kappa}}\}$, which replaces the momentum gradient $\nabla_{\mathbf{p}} f$ in the Boltzmann equation, will be detailed in the next subsection.

The equilibrium functions $f_{\boldsymbol{\kappa}}^{eq} \equiv f^{eq}(\mathbf{x}, \mathbf{p}_{\boldsymbol{\kappa}}, t)$ are given by [34, 35]:

$$f_{\boldsymbol{\kappa}}^{eq} = n \prod_{\alpha=1}^D g_{k_\alpha}, \quad (5)$$

where

$$g_{k_\alpha} \equiv g_{k_\alpha}(u_\alpha(\mathbf{x}, t), T(\mathbf{x}, t)) = w_{k_\alpha} \sum_{\ell=0}^N H_\ell(p_{k_\alpha}) \sum_{s=0}^{\lfloor \ell/2 \rfloor} \frac{(mT-1)^s (mu_\alpha)^{\ell-2s}}{2^s s! (\ell-2s)!}, \quad (6)$$

and $\lfloor \ell/2 \rfloor$ is the integer part of $\ell/2$. To each $p_{k_\alpha} \in \{\mathcal{R}_q\}$, $k_\alpha = 1, 2, \dots, Q$, $\alpha \in \{1, 2\}$, there is an associated weight $w_{k_\alpha} \in \{\mathcal{W}_q\}$, given by Eq. (2) and we will use the notation $w_{\boldsymbol{\kappa}} \equiv w_{k_1 k_2} = w_{k_1} w_{k_2}$.

2.2. Force term

The following expression of the force $\mathbf{F} \equiv \mathbf{F}(\mathbf{x}, t)$, which appears in Eq.(4), was used in order to simulate the evolution of a van der Waals fluid [4, 44, 45, 46, 47, 48]:

$$\mathbf{F} = \frac{1}{n} \nabla(p^i - p^w) + \sigma \nabla(\Delta n). \quad (7)$$

In this expression, the parameter σ controls the surface tension, $p^i = nT$ is the ideal gas pressure and the nondimensionalised form of the van der Waals equation of state reads

$$p^w = \frac{3nT}{3-n} - \frac{9}{8}n^2, \quad (8)$$

where the values of the particle number density and temperature in the critical point are $n_c = 1$ and $T_c = 1$, respectively. A 25-point stencil is used to compute the two Cartesian components of the force \mathbf{F} in each lattice node \mathbf{x} at time t [48, 49, 50].

To account for the Cartesian components $(\partial_{p_\alpha} f)_{\boldsymbol{\kappa}}$, $\alpha \in \{1, 2\}$ of $\{(\nabla_{\mathbf{p}} f)_{\boldsymbol{\kappa}}\}$, which appear in Eq.(4), we first expand the single particle distribution function $f(\mathbf{x}, \mathbf{p}, t)$ with respect to the full-range Hermite polynomials $H_\ell(p_\alpha)$ defined on the Cartesian axis $\alpha \in \{1, 2\}$ of the momentum space, to get [35]:

$$f(\mathbf{x}, \mathbf{p}, t) = \frac{1}{\sqrt{2\pi}} e^{-p_\alpha^2/2} \sum_{\ell=0}^{\infty} \frac{1}{\ell!} \mathcal{F}_{\alpha, \ell}(\mathbf{x}, p_{\bar{\alpha}}, t) H_\ell(p_\alpha), \quad (9)$$

where

$$\mathcal{F}_{\alpha, \ell}(\mathbf{x}, p_{\bar{\alpha}}, t) = \int_{-\infty}^{\infty} f(\mathbf{x}, \mathbf{p}, t) H_\ell(p_\alpha) dp_\alpha, \quad (10)$$

$$\bar{\alpha} = \begin{cases} 2, & \alpha = 1 \\ 1, & \alpha = 2 \end{cases} \quad (11)$$

Using the recurrence property of the Hermite polynomials $\partial_x[e^{-x^2/2}H_\ell(x)] = -e^{-x^2/2}H_{\ell+1}(x)$ [11, 35] to compute the derivative with respect to p_α of $f(\mathbf{x}, \mathbf{p}, t)$ given in Eq. (9), we get

$$\partial_{p_\alpha} f(\mathbf{x}, \mathbf{p}, t) = -\frac{1}{\sqrt{2\pi}} e^{-p_\alpha^2/2} \sum_{\ell=0}^{\infty} \frac{1}{\ell!} \mathcal{F}_{\alpha, \ell}(\mathbf{x}, p_{\bar{\alpha}}, t) H_{\ell+1}(p_\alpha). \quad (12)$$

After truncation of this expression up to order N , the application of the discretisation procedure in the momentum space gives:

$$(\partial_{p_\alpha} f)_\kappa \equiv (\partial_{p_\alpha} f)_\kappa(\mathbf{x}, t) = -w_{k_\alpha} \sum_{\ell=0}^{N-1} \frac{1}{\ell!} \mathcal{F}_{\alpha, \ell; k_{\bar{\alpha}}}(\mathbf{x}, t) H_{\ell+1}(p_{k_\alpha}), \quad (13)$$

$$\mathcal{F}_{\alpha, \ell; k_{\bar{\alpha}}}(\mathbf{x}, t) = \sum_{k_\alpha=1}^Q f_\kappa(\mathbf{x}, t) H_\ell(p_{k_\alpha}). \quad (14)$$

45 Note that the sum in Eq.(13) above runs up to $\ell = N-1$ since $H_{N+1}(p_{k_\alpha}) = 0$ for all $k_\alpha = 1, 2, \dots, Q = N+1$, $\alpha \in \{1, 2\}$.

2.3. Macroscopic equations

Multiplying the Boltzmann equation (4) with the collision invariants 1, \mathbf{p} and $\mathbf{p}^2/2m$ and integrating over the momentum space yields the following macroscopic equations:

$$\partial_t n + \nabla \cdot (n\mathbf{u}) = 0, \quad (15a)$$

$$\rho [\partial_t u_\alpha + (\mathbf{u} \cdot \nabla) u_\alpha] = n F_\alpha - \partial_\alpha p^i - \partial_\beta \Pi_{\alpha\beta}, \quad (15b)$$

$$n [\partial_t T + (\mathbf{u} \cdot \nabla) T] + \partial_\alpha q_\alpha + p^i (\nabla \cdot \mathbf{u}) + \Pi_{\alpha\beta} \partial_\alpha u_\beta = 0, \quad (15c)$$

where $\Pi_{\alpha\beta}$ is the viscous part of the stress tensor and q_α is the heat flux, defined in terms of the peculiar momentum $\boldsymbol{\xi} = \mathbf{p} - m\mathbf{u}$ as follows:

$$\Pi_{\alpha\beta} + p^i \delta_{\alpha\beta} = \int d^2 p f \frac{\xi_\alpha \xi_\beta}{m}, \quad q_\alpha = \int d^2 p f \frac{\boldsymbol{\xi}^2 \xi_\alpha}{2m m}. \quad (16)$$

The force (7) has the effect of replacing the ideal gas pressure p^i in the momentum equation (15b) with the van der Waals momentum p^w , while also adding a surface tension term:

$$\rho [\partial_t u_\alpha + (\mathbf{u} \cdot \nabla) u_\alpha] = \sigma \nabla \cdot (\Delta n) - \partial_\alpha p^w - \partial_\beta \Pi_{\alpha\beta}. \quad (17)$$

The above modification to the momentum equation is sufficient to induce spontaneous phase separation when the temperature T of the fluid is smaller than the critical temperature T_c .

Furthermore, a Chapman-Enskog analysis shows that, at first order, the viscous stress tensor and the heat flux are given by [39]:

$$\Pi_{\alpha\beta} = -\eta (\partial_\alpha u_\beta + \partial_\beta u_\alpha - \delta_{\alpha\beta} \nabla \cdot \mathbf{u}), \quad q_\alpha = -\kappa_T \nabla_\alpha T, \quad (18)$$

where the dynamic viscosity η and heat conductivity κ_T have the following expressions:

$$\eta = \tau n T, \quad \kappa_T = \frac{2}{m} \tau n T. \quad (19)$$

The ensuing Prandtl number $\text{Pr} = c_p \eta / \kappa_T$ ($c_p = 2/m$ is the specific heat) is fixed in the BGK model at:

$$\text{Pr} = 1, \quad (20)$$

50 while the hard sphere model predicts that $\text{Pr} = 2/3$.

Given the above mentions there are two remarks we want to highlight: first, since the phase separation mechanism is induced through the use of a body force, the pressure appearing in the energy equation (15c) is still the ideal pressure, instead of the van der Waals pressure [51]; and second, the value of Pr (20) is fixed at 1. The energy equation could be altered such that the ideal fluid pressure is replaced by the van der Waals pressure by employing the modified Boltzmann (i.e. Enskog) equation [52]. Furthermore, there are various methods to alter the value of Pr , of which we mention the Shakhov model [39] and the MRT model [53, 54]. These possible enhancements are the subject of forthcoming work. In this paper, we are interested to perform a first exploration of the capabilities of the single particle distribution function LB model based on Gauss-Hermite quadratures to simulate liquid-vapour thermal flows and, for simplicity, we only considered the simple form of both the body force term and of the collision term in Eq. (4).

2.4. Numerical scheme

For $Q > 3$, the roots \mathcal{R}_q , $1 \leq q \leq Q$ of the probabilists' Hermite polynomial of order Q are irrational. Hence, the corresponding LB models are *off-lattice*, i.e., the vectors in the discrete momentum set do not point from a lattice node to another. In this case, the *streaming procedure* [4, 32, 44] can no longer be used to evolve the functions $f_\kappa \equiv f_\kappa(\mathbf{x}, t)$ according to Eq.(4). To evolve these functions, in this paper we use a flux limiter projection method [39, 55, 56, 57, 58], which is briefly outlined below.

For every f_κ defined in the node x of the $2D$ square lattice, we associate the *in* and *out* fluxes along each Cartesian axis $\alpha \in \{1, 2\}$:

$$\mathfrak{F}_{\kappa,\alpha}^{\text{out}}(\mathbf{x}, t) = \frac{|p_{k_\alpha}|}{m} \left\{ f_\kappa(\mathbf{x}, t) + \frac{1}{2m} \left(1 - \frac{|p_{k_\alpha}| \delta t}{m \delta x} \right) [f_{\kappa,\alpha}^+(\mathbf{x}, t) - f_\kappa(\mathbf{x}, t)] \Psi(\theta_{\kappa,\alpha}(\mathbf{x}, t)) \right\}, \quad (21)$$

$$\mathfrak{F}_{\kappa,\alpha}^{\text{in}}(\mathbf{x}, t) = \mathfrak{F}_{\kappa,\alpha}^{\text{out}}(\mathbf{x} - \text{sgn}(p_{k_\alpha}) \delta s \mathbf{e}_\alpha, t), \quad (22)$$

where δs is the lattice spacing, δt is the time step, \mathbf{e}_α is the unit vector on the Cartesian axis α and

$$f_{\kappa,\alpha}^\pm(\mathbf{x}, t) = f_\kappa(\mathbf{x} \pm \text{sgn}(p_{k_\alpha}) \delta s \mathbf{e}_\alpha, t), \quad (23)$$

$$\text{sgn}(p_{k_\alpha}) = \begin{cases} -1 & , \quad p_{k_\alpha} < 0 \\ 0 & , \quad p_{k_\alpha} = 0 \\ 1 & , \quad p_{k_\alpha} > 0. \end{cases} \quad (24)$$

In this paper we use the *MCD* flux limiter [47, 57, 58, 59]

$$\Psi(\theta) = \begin{cases} 0 & , \quad \theta \leq 0 \\ 2\theta & , \quad 0 < \theta \leq 1/3 \\ (1 + \theta)/2 & , \quad 1/3 < \theta \leq 3 \\ 2 & , \quad 3 < \theta, \end{cases} \quad (25)$$

which is a function of the smoothness

$$\theta \equiv \theta_{\kappa,\alpha}(\mathbf{x}, t) = \frac{f_\kappa(\mathbf{x}, t) - f_{\kappa,\alpha}^-(\mathbf{x}, t)}{f_{\kappa,\alpha}^+(\mathbf{x}, t) - f_\kappa(\mathbf{x}, t)}. \quad (26)$$

Note that in the particular case $\Psi(\theta) = 0$, the flux limiter scheme reduces to the first order upwind scheme [57, 58]. In the bulk nodes of the lattice, as well as in those nodes where periodic boundary conditions apply, the functions f_κ are updated according to

$$f_\kappa(\mathbf{x}, t + \delta t) = f_\kappa(\mathbf{x}, t) - \sum_{\alpha=1}^2 \frac{\delta t}{\delta s} [\mathfrak{F}_{\kappa,\alpha}^{\text{out}}(\mathbf{x}, t) - \mathfrak{F}_{\kappa,\alpha}^{\text{in}}(\mathbf{x}, t)] - \frac{\delta t}{\tau} [f_\kappa(\mathbf{x}, t) - f_\kappa^{eq}(\mathbf{x}, t)] - \sum_{\alpha=1}^2 \delta t F_\alpha \cdot \nabla_{p_{k_\alpha}} f_\kappa. \quad (27)$$

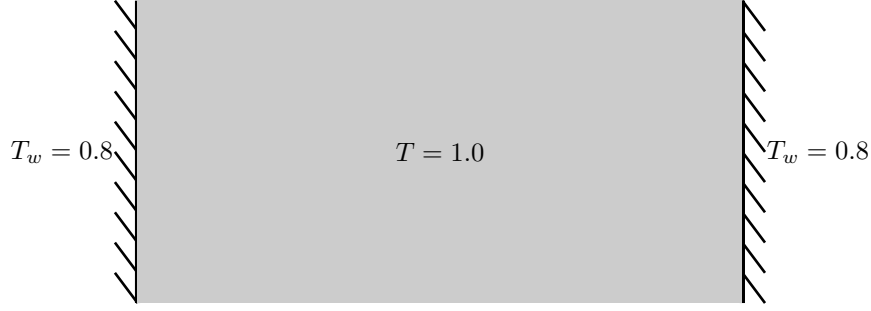


Figure 1: Initial setup.

2.5. Boundary conditions

In this paper, we consider the phase separation in a van der Waals fluid placed between two parallel walls. Figure 1 shows the initial setup of the problem. At time $t=0$, we always start with a fluid at rest in local thermal equilibrium, whose temperature equals the critical temperature $T_c = 1.0$. The initial value of the particle number density in the lattice nodes fluctuates around the critical value $n_c = 1$ with random deviations of at most $0.01 \times n_c$. The fluid is placed between two parallel walls at rest ($\mathbf{u}_w = 0$), which are perpendicular to the horizontal axis. The temperature of the walls is set to $T_w < T_c$ and kept constant throughout the simulation. In this arrangement, the energy is extracted through the walls and the liquid and vapor phases start to separate. This process is allowed by implementing the diffuse reflection boundary conditions on the walls, as summarized below [34, 39, 55, 56, 60, 61].

According to the diffuse reflection concept, the distribution function of the fluid particles that return from the wall is the Maxwell-Boltzmann equilibrium distribution function corresponding to the wall velocity \mathbf{u}_w and temperature T_w . For convenience, let us consider a $2D$ square lattice with $\mathfrak{N}_1 \times \mathfrak{N}_2$ nodes and let $\mathbf{x} = i\delta s\mathbf{e}_1 + j\delta s\mathbf{e}_2$, $1 \leq i \leq \mathfrak{N}_1$, $1 \leq j \leq \mathfrak{N}_2$, be the position vectors of the nodes in this lattice. Specialising to the left wall in Figure 1, all nodes $\mathbf{x}_{i,j}$ with $i = 1$ and $1 \leq j \leq \mathfrak{N}_2$, are situated near this wall. According to Eq. (21), the particle flux that originates from the node $\mathbf{x}_{1,j}$ and hits the wall in the normal direction, $\alpha = 1$, is

$$\begin{aligned}
\mathfrak{F}_w^{out}(\mathbf{x}_{1,j}, t) &= \sum_{\substack{k_x=1 \\ p_{k_x} < 0}}^Q \sum_{k_y=1}^Q \mathfrak{F}_{\kappa, \mathbf{x}}^{out}(\mathbf{x}_{1,j}, t) \\
&= \sum_{\substack{ck_1=1 \\ p_{k_1} < 0}}^Q \sum_{k_2=1}^Q \frac{p_{k_1}}{m} \left\{ f_{k_1 k_2}(\mathbf{x}_{1,j}, t) + \frac{1}{2m} \left(1 - \frac{|p_{k_1}| \delta t}{m \delta x} \right) \times \right. \\
&\quad \left. \left[f_{k_1 k_2}(\mathbf{x}_{1,j}, t) - f_{k_1 k_2}(\mathbf{x}_{0,j}, t) \right] \Psi \left(\frac{f_{k_1 k_2}(\mathbf{x}_{2,j}, t) - f_{k_1 k_2}(\mathbf{x}_{1,j}, t)}{f_{k_1 k_2}(\mathbf{x}_{1,j}, t) - f_{k_1 k_2}(\mathbf{x}_{0,j}, t)} \right) \right\}, \quad (28)
\end{aligned}$$

where the function $f_{k_1 k_2}(\mathbf{x}_{0,j}, t)$, defined in the first ghost node outside the wall, is found by a linear extrapolation procedure that sets both the smoothness and the flux limiter Ψ in Eq. (28) equal to unity:

$$f_{k_1 k_2}(\mathbf{x}_{0,j}, t) = 2f_{k_1 k_2}(\mathbf{x}_{1,j}, t) - f_{k_1 k_2}(\mathbf{x}_{2,j}, t). \quad (29)$$

According to the diffuse reflection concept, the particle flux returning from the wall is Maxwellian:

$$\mathfrak{F}_{\kappa, \mathbf{x}}^{in}(\mathbf{x}_1, t) = n_w \frac{p_{k_1}}{m} g_{k_1}(u_w, T_w) g_{k_2}(u_w, T_w). \quad (30)$$

The value of n_w in the expression of $\mathfrak{F}_{\kappa, \mathbf{x}}^{in}$ above is found for each value of j by requiring the total flux of particles to vanish at the wall:

$$\mathfrak{F}_w^{out} + \mathfrak{F}_w^{in} = 0, \quad (31)$$

where

$$\mathfrak{F}_w^{in}(\mathbf{x}_{1,j}, t) = \sum_{\substack{k_1=1 \\ p_{k_1}>0}}^Q \sum_{k_2=1}^Q \mathfrak{F}_{\kappa,x}^{in}(\mathbf{x}_1, t) = n_w \sum_{\substack{k_1=1 \\ p_{k_1}>0}}^Q \sum_{k_2=1}^Q \frac{p_{k_1}}{m} g_{k_1}(u_w, T_w) g_{k_2}(u_w, T_w). \quad (32)$$

Finally, in order to compute the fluxes $\mathfrak{F}_{\kappa,x}^{out}(\mathbf{x}_{1,j}, t)$ and $\mathfrak{F}_{\kappa,x}^{in}(\mathbf{x}_{2,j}, t)$ for $p_{k_x} > 0$, the value of $f_{\kappa}(\mathbf{x}_{0,j}, t)$ must be specified. Since we assume that the particles emerging from the wall towards the fluid domain is Maxwellian, we set

$$f_{\kappa}(\mathbf{x}_{0,j}, t) = n_w g_{k_1}(u_w, T_w) g_{k_2}(u_w, T_w). \quad (33)$$

3. Computer results

Figure 2 shows the evolution of the liquid - vapor separation process on a 1024×512 lattice. At $t = 0$, the fluid temperature was $T = T_c = 1.0$ and the wall temperature was set to $T_w = 0.8$. The simulation was conducted with the time step $\delta t = 10^{-5}$ and the lattice spacing $\delta s = 1/512$. At early times, one observes the liquid deposition on the cold walls. As the bulk temperature decreases, further parallel bands of low and high density appear near the walls. Afterwards, these bands break into individual droplets due to the action of surface tension. The formation of liquid droplets in the central region of the channel is observed at later stages of the simulation. This happens because the temperature in the center of the channel decreases during the heat extraction through the walls, but always remains higher than the wall temperature, as seen in the right column of Figure 2. This feature was observed also when investigating the liquid-vapour phase separation with a different thermal LB model [12]. Moreover, the right column of Figure 2 revealed that the local maxima in the temperature profiles are located in the liquid-vapour interface regions. In these regions, where large density gradients are present, there is an unphysical heat generation process, due to the spurious velocity, a numerical effect that plagues the LB models [5, 62, 63, 64, 65, 66, 67, 68, 69, 70, 71]. In general, this numerical effect can be reduced by using very elaborated higher order numerical schemes [63], or smaller values of the time step δt and/or the lattice spacing δs .

To investigate the effect of δt and δs on the accuracy of our LB model, we considered a fully separated (stationary) liquid-vapour-liquid system placed between two parallel walls at temperature $T_w = 0.8$. In order to reduce the computational costs, in the sequel we narrowed the simulation domain to only 16 nodes on the y axis.

Figure 3a shows the maximum value of the spurious velocity as a function of the lattice spacing δs , for the time step $\delta t = 10^{-5}$. A quite linear dependence with respect to δt is observed. Figure 3b shows the same quantity as a function of the time step δt for the lattice spacing $\delta s = 1/256$. This figure shows a quadratic dependence of the maximum spurious velocity on the lattice spacing. In Figure 4a we plotted the temperature difference $\Delta T = T_{max} - T_w$ between the maximum temperature T_{max} in the channel and the wall temperature T_w versus the time step δt , for the lattice spacing $\delta s = 1/256$. One can see that the temperature difference ΔT increases monotonically with the time step δt . Figure 4b shows the dependence of ΔT vs the lattice spacing δs , for the time step $\delta t = 10^{-5}$. The dependence of ΔT becomes stronger for larger values of δs , when the numerical effect induced by this quantity prevails over the numerical effect of the time step δt .

Further investigations performed with $\delta s = 1/1024$, $\delta t = 10^{-6}$ and three values of the wall temperature are shown in Figure 5. As seen in Figure 5 the magnitude of the spurious velocity is larger when the wall temperature is lower and the density gradient in the interface region increases. In the stationary state the local maxima of the temperature difference ΔT are below 1.0% of the wall temperature T_w .

Figure 6 shows the liquid-vapour phase diagram, as recovered with our model using the same conditions as in Figure 5. The values of the density are collected from the first lattice node near the wall for the liquid phase (ρ_ℓ) and from the center of the channel for the vapour phase (ρ_v). Very good agreement is observed between the density values obtained with our model and those obtained through the Maxwell construction.

115 4. Conclusion

A single particle distribution function thermal lattice Boltzmann model based on the full-range Gauss-Hermite quadrature of order $Q = 5$ was tested by simulating the liquid-vapour phase separation in a van der Waals fluid bounded by two parallel walls. A third order 25-point stencil for the computation of the van der Waals force term. We validated our thermal model by comparing the phase separation results against
120 the Maxwell construction results. Good agreement was obtained for temperatures as low as $0.7 T_c$.

Starting from an initial state in which the fluid is at the critical temperature T_c , with random density fluctuations of at most 1% around the critical density, we investigated the phase separation between two walls kept at a constant temperature $T_w < T_c$. Our simulations show that the condensation starts in the vicinity of the walls. As the bulk temperature decreases, liquid droplets develop further in the channel. We observed
125 that in the stationary state, spurious currents persist, which affect the temperature field through spurious heating at the vapour-liquid interface. To avoid the large relative errors induced by the numerical effects, it is necessary to use the second order flux limiter scheme with sufficiently small values of the lattice spacing δs and the time step δt , e.g. $(\delta s, \delta t) = (1/1024, 10^{-6})$. With these parameters, the non-dimensionalised magnitude of the spurious velocity is below 6×10^{-5} , while the fluid temperature profile is within the range
130 of 1.0% above the wall temperature T_w , even when $T_w = 0.7 T_c$.

Acknowledgments

This work is supported by a grant from the Romanian National Authority for Scientific Research, CNCS-UEFISCDI, project number PN-II-ID-PCE-2011-3-0516. VEA gratefully acknowledges the support of NVIDIA Corporation with the donation of one of the Tesla K40 GPUs used for this research. The authors
135 are indebted to Adrian Horga for invaluable insight regarding the development of our CUDA code.

References

- [1] F. Massaioli, R. Benzi, S. Succi, Exponential tails in 2-dimensional Rayleigh-Benard convection, *Europhysics Letters* 21 (1993) 305–310. doi:10.1209/0295-5075/21/3/009.
- [2] F. Alexander, S. Chen, J. Sterling, Lattice Boltzmann thermohydrodynamics, *Physical Review E* 47 (1993) R2249–R2252.
- 140 [3] Y. Qian, Simulating thermohydrodynamics with lattice BGK models, *Journal of Scientific Computing* 8 (1993) 231–242.
- [4] Z. Guo, C. Shu, *Lattice Boltzmann Method and its Applications in Engineering*, World Scientific Publishing Co. Pte. Ltd., Singapore, 2013.
- [5] Q. Li, K. Luo, Q. Kang, Y.L.He, Q.Chen, Q.Liu, Lattice Boltzmann methods for multiphase flow and phase-change heat transfer, *Progress in Energy and Combustion Science* 52 (2016) 62–105. doi:10.1016/j.pecs.2015.10.001.
- 145 [6] Y.Chen, H. Ohashi, M. Akiyama, Thermal lattice Bhatnagar-Gross-Krook model without nonlinear deviations in macrodynamics equations, *Physical Review E* 50 (2015) 2776–2783. doi:10.1103/PhysRevE.50.2776.
- [7] M. Watari, M. Tsutahara, Two-dimensional thermal model of the finite-difference lattice Boltzmann method with high spatial isotropy, *Physical Review E* 67 (2003) 036306. doi:10.1103/PhysRevE.67.036306.
- [8] M. Watari, M. Tsutahara, Possibility of constructing a multispeed Bhatnagar-Gross-Krook thermal model of the lattice Boltzmann method, *Physical Review E* 70 (2004) 016703. doi:10.1103/PhysRevE.70.016703.
- 150 [9] V. Sofonea, R. F. Sekerka, Diffuse-reflection boundary conditions for a thermal lattice Boltzmann model in two dimensions: Evidence of temperature jump and slip velocity in micro channels, *Phys. Rev. E* 71 (2005) 066709. doi:10.1103/PhysRevE.71.066709.
- [10] P. Philippi, L. Hegele, Jr., L.O.E. dos Santos, R. Surmas, From the continuous to the lattice Boltzmann equation: The discretization problem and thermal models, *Physical Review E* 73 (2006) 056702. doi:10.1103/PhysRevE.73.056702.
- 155 [11] X. W. Shan, X. F. Yuan, H. D. Chen, Kinetic theory representation of hydrodynamics: a way beyond the Navier-Stokes equation, *J. Fluid. Mech.* 550 (2006) 413–441. doi:10.1017/S0022112005008153.
- [12] G. Gonnella, A. Lamura, V. Sofonea, Lattice Boltzmann simulation of thermal non ideal fluids, *Phys. Rev. E* 76 (2007) 036703. doi:10.1103/PhysRevE.76.036703.
- 160 [13] M. Sbragaglia, R. Benzi, L. Biferale, H. Chen, X. Shan, S. Succi, Lattice Boltzmann method with self-consistent thermohydrodynamic equilibria, *Journal of Fluid Mechanics* 628 (2009) 299–309. doi:10.1017/S002211200900665X.
- [14] F. Chen, A. X. G. Zhang, Y.J.Li, S. Succi, Multiple-relaxation-time lattice Boltzmann approach to compressible flows with flexible specific-heat ratio and prandtl number, *EPL* 90 (2010) 54003. doi:10.1209/0295-5075/90/54003.
- [15] N. Frapolli, S. Chikatamarla, I. Karlin, Multispeed entropic lattice Boltzmann model for thermal flows, *Physical Review E* 90 (2014) 043306. doi:10.1103/PhysRevE.90.043306.
- 165 [16] X. He, S. Chen, G. Doolen, A novel thermal model for the lattice Boltzmann method in incompressible limit, *Journal of Computational Physics* 146 (1998) 282–300. doi:10.1006/jcph.1998.6057.

- [17] Z. Guo, C. Zheng, B. Shi, T. Zhao, Thermal lattice Boltzmann equation for low mach number flows: Decoupling model, *Physical Review E* 75 (2007) 036704. doi:10.1103/PhysRevE.75.036704.
- 170 [18] Y. Zhang, X. Gu, R. Barber, D. Emerson, Modelling thermal flow in the transition regime using a lattice Boltzmann approach, *EPL* 77 (2007) 30003. doi:10.1209/0295-5075/77/30003.
- [19] I. Karlin, D. Sichau, S. Chikatamarla, Consistent two-population lattice Boltzmann model for thermal flows, *Physical Review E* 88 (2013) 063310. doi:10.1103/PhysRevE.88.063310.
- [20] H. Yasuoka, M. Kaneda, K. Suga, Thermal lattice Boltzmann method for complex microflows, *Physical Review E* 94 (2016) 013102. doi:10.1103/PhysRevE.94.013102.
- 175 [21] G. Pareschi, N. Frapolli, S. Chikatamarla, I. Karlin, Conjugate heat transfer with the entropic lattice Boltzmann method, *Physical Review E* 94 (2016) 013305. doi:10.1103/PhysRevE.94.013305.
- [22] R. Zhang, H. Chen, Lattice Boltzmann method for simulations of liquid-vapor thermal flows, *Phys. Rev. E* 67 (2003) 066711. doi:10.1103/PhysRevE.67.066711.
- 180 [23] P. Lallemand, L. Luo, Hybrid finite-difference thermal lattice Boltzmann equation, *International Journal of Modern Physics B* 17 (2003) 41–47. doi:10.1142/S0217979203017060.
- [24] P. Lallemand, L. Luo, Theory of the lattice Boltzmann method: Acoustic and thermal properties in two and three dimensions, *Physical Review E* 68 (2003) 036706. doi:10.1103/PhysRevE.68.036706.
- [25] G. Gonnella, A. Lamura, A. Piscitelli, A. Tiribocchi, Phase separation of binary fluids with dynamic temperature, *Physical Review E* 82 (2010) 046302. doi:10.1103/PhysRevE.82.046302.
- 185 [26] H. Safari, M. Rahimian, M. Krafczyk, Extended lattice Boltzmann method for numerical simulation of thermal phase change in two-phase fluid flow, *Physical Review E* 88 (2013) 013304. doi:10.1103/PhysRevE.88.013304.
- [27] H. Safari, M. Rahimian, M. Krafczyk, Consistent simulation of droplet evaporation based on the phase-field multiphase lattice Boltzmann method, *Physical Review E* 90 (2014) 033305. doi:10.1103/PhysRevE.90.033305.
- 190 [28] Z. Li, M. Yang, Y.W.Zhang, Hybrid lattice Boltzmann and finite volume method for natural convection, *Journal of Thermophysics and Heat Transfer* 28 (2014) 68–77. doi:10.2514/1.T4211.
- [29] Q. Li, Q. Kang, M.M.Francois, Y.L.He, K.H.Luo, Lattice Boltzmann modeling of boiling heat transfer: The boiling curve and the effects of wettability, *International Journal of Heat and Mass Transfer* 85 (2015) 787–796. doi:10.1016/j.ijheatmasstransfer.2015.01.136.
- 195 [30] International Conference for Mesoscopic Methods in Engineering and Science (ICMMES), URL: www.icmmes.org.
- [31] International Conference on Discrete Simulation in Fluid Dynamics (DSFD), URL: www.dsfd.org.
- [32] M. O. Deville, T. B. Gatski, *Mathematical Modeling for Complex Fluids and Flows*, Springer, Berlin, 2012.
- [33] P. Fede, V. Sofonea, R. Fournier, S. Blanco, O. Simonin, G. Lepoutère, V. E. Ambruş, Lattice Boltzmann model for predicting the deposition of inertial particles transported by a turbulent flow, *Int. J. Multiph. Flow* 76 (2015) 187–197. doi:10.1016/j.ijmultiphaseflow.2015.07.004.
- 200 [34] V. E. Ambruş, V. Sofonea, Lattice Boltzmann models based on half-range Gauss-Hermite quadratures, *J. Comput. Phys.* 316 (2016) 760–788. doi:10.1016/j.jcp.2016.04.010.
- [35] V. E. Ambruş, V. Sofonea, Application of mixed quadrature lattice Boltzmann models for the simulation of Poiseuille flow at non-negligible values of the Knudsen number, *J. Comput. Sci.* doi:10.1016/j.jocs.2016.03.016.
- 205 [36] B. Piaud, S. Blanco, R. Fournier, V. E. Ambruş, V. Sofonea, Gauss quadratures - the keystone of lattice Boltzmann models, *Int. J. Mod. Phys. C* 25 (2014) 1340016. doi:10.1142/S0129183113400160.
- [37] S. Chikatamarla, I. Karlin, Lattices for the lattice Boltzmann method, *Physical Review E* 79 (2009) 046701. doi:10.1103/PhysRevE.79.046701.
- [38] J. Shim, R. Gatignol, Thermal lattice Boltzmann method based on a theoretical simple derivation of the Taylor expansion, *Physical Review E* 83 (2011) 046710. doi:10.1103/PhysRevE.83.046710.
- 210 [39] V. E. Ambruş, V. Sofonea, High-order thermal lattice Boltzmann models derived by means of Gauss quadrature in the spherical coordinate system, *Phys. Rev. E* 86 (2012) 016708. doi:10.1103/PhysRevE.86.016708.
- [40] B. Shizgal, *Spectral Methods in Chemistry and Physics: Applications to Kinetic Theory and Quantum Mechanics (Scientific Computation)*, Springer, 2015.
- 215 [41] F. B. Hildebrand, *Introduction to Numerical Analysis*, second edition Edition, Dover Publications, 1987.
- [42] M. Abramowitz, I. A. Stegun, *Handbook of mathematical functions with formulas, graphs and mathematical tables*, tenth printing Edition, National Bureau of Standards, Washington, 1972.
- [43] F. W. J. Olver, D. W. Lozier, R. F. Boisvert, C. W. Clark, *NIST Handbook of Mathematical Functions*, Cambridge University Press, New York, 2010.
- 220 [44] H. Huang, M. Sukop, X. Lu, *Multiphase Lattice Boltzmann Methods: Theory and Applications*, John Wiley & Sons, Ltd., Chichester, UK, 2015.
- [45] X. He, X. Shan, G. Doolen, Discrete Boltzmann equation model for nonideal gases, *Physical Review E* 57 (1998) R13. doi:10.1103/PhysRevE.57.R13.
- [46] L. Luo, Unified theory of lattice Boltzmann models for nonideal gases, *Physical Review Letters* 81 (1998) 1618. doi:10.1103/PhysRevLett.81.1618.
- 225 [47] V. Sofonea, A. Lamura, G. Gonnella, A. Cristea, Finite-difference lattice Boltzmann model with flux limiters for liquid-vapor systems, *Phys. Rev. E* 70 (2004) 046702. doi:10.1103/PhysRevE.70.046702.
- [48] T. Biciuşcă, A. Horga, V. Sofonea, Simulation of liquid-vapour phase separation on GPUs using Lattice Boltzmann models with off-lattice velocity sets, *Comptes Rendus Mécanique* 343 (2015) 580–588. doi:10.1016/j.crme.2015.07.011.
- 230 [49] S. Leclaire, M. El-Hachem, J. Trepanier, M.Reggio, High order spatial generalization of 2d and 3d isotropic discrete gradient operators with fast evaluation on gpus, *JOURNAL OF SCIENTIFIC COMPUTING* 59 (3) (2014) 545–573. doi:10.1007/s10915-013-9772-2.

- [50] M. Patra, M. Karttunen, Stencils with isotropic discretization error for differential operators, *NUMERICAL METHODS FOR PARTIAL DIFFERENTIAL EQUATIONS* 22 (4) (2006) 936–953. doi:10.1002/num.20129.
- 235 [51] L.-S. Luo, Theory of the lattice Boltzmann method: Lattice Boltzmann models for nonideal gases, *Phys. Rev. E* 62 (2000) 4982–4996. doi:10.1103/PhysRevE.62.4982.
- [52] X. He, G. D. Doolen, Thermodynamic foundations of kinetic theory and lattice Boltzmann models for multiphase flows, *Jour. of Stat. Phys.* 107 (112) (2002) 309–328. doi:10.1023/A:1014527108336.
- 240 [53] G. R. McNamara, A. L. Garcia, B. J. Alder, Stabilization of thermal lattice Boltzmann models, *J. Stat. Phys* 81 (1995) 395–408. doi:10.1007/BF02179986.
- [54] F. Chen, A. Xu, G. Zhang, Y. Li, S. Succi, Multiple-relaxation-time lattice Boltzmann approach to compressible flows with flexible specific-heat ratio and Prandtl number, *EPL* 90 (2010) 54003. doi:10.1209/0295-5075/90/54003.
- [55] J. P. Meng, Y. H. Zhang, Gauss-Hermite quadratures and accuracy of lattice Boltzmann models for nonequilibrium gas flows, *Phys. Rev. E* 83 (2011) 036704. doi:10.1103/PhysRevE.83.036704.
- 245 [56] J. P. Meng, Y. H. Zhang, X. W. Shan, Multiscale lattice Boltzmann approach to modeling gas flows, *Phys. Rev. E* 83 (2011) 046701. doi:10.1103/PhysRevE.83.046701.
- [57] R. J. LeVeque, *Finite Volume Methods for Hyperbolic Problems*, Cambridge University Press, Cambridge, 2002.
- [58] E. Toro, *Riemann Solvers and Numerical Methods for Fluid Dynamics*, Springer, Berlin, 1999.
- 250 [59] A. Cristea, V. Sofonea, Two component lattice Boltzmann model with flux limiters, *Central European Journal of Physics* 2 (2004) 382. doi:10.2478/BF02475638.
- [60] S. Ansumali, I. Karlin, Kinetic boundary conditions in the lattice Boltzmann method, *Phys. Rev. E* 66 (2002) 026311. doi:10.1103/PhysRevE.66.026311.
- [61] V. Sofonea, Implementation of diffuse reflection boundary conditions in a thermal lattice Boltzmann model with flux limiters, *J. Comput. Phys.* 228 (2009) 6107–6118. doi:10.1016/j.jcp.2009.05.009.
- 255 [62] A. Zarghami, N. Looije, H. Van den Akker, Assessment of interaction potential in simulating nonisothermal multiphase systems by means of lattice Boltzmann modeling, *Physical Review E* 92 (2015) 023307. doi:10.1103/PhysRevE.92.023307.
- [63] K. Hejranfar, E. Ezzatneshan, Simulation of two-phase liquid vapor flows using a high-order compact finite-difference lattice Boltzmann method, *Physical Review E* 92 (2015) 053305. doi:10.1103/PhysRevE.92.053305.
- [64] L. Chen, Q. Kang, Y. Mu, Y. He, W. Tao, A critical review of the pseudopotential multiphase lattice Boltzmann model: Methods and applications, *International Journal of Heat and Mass Transfer* 76 (2014) 210–236. doi:10.1016/j.ijheatmasstransfer.2014.04.032.
- 260 [65] S. Khajepour, B. Chen, Multipseudopotential interaction: A solution for thermodynamic inconsistency in pseudopotential lattice Boltzmann models, *Physical Review E* 91 (2015) 023301. doi:10.1103/PhysRevE.91.023301.
- [66] S. Khajepour, B. Chen, Multipseudopotential interaction: A consistent study of cubic equations of state in lattice Boltzmann models, *Physical Review E* 93 (2016) 013303. doi:10.1103/PhysRevE.93.013303.
- 265 [67] M. Ikeda, P. Rao, L. Schaefer, A thermal multicomponent lattice Boltzmann model, *Computers and Fluids* 101 (2014) 250–262. doi:10.1016/j.compfluid.2014.06.006.
- [68] Y. Gan, A. Xu, G. Zhang, Fft-lb modeling of thermal liquid-vapor system, *Communications in Theoretical Physics* 57 (2012) 681–694. doi:10.1088/0253-6102/57/4/24.
- 270 [69] Y. Gan, A. Xu, G. Zhang, Y. Li, Physical modeling of multiphase flow via lattice Boltzmann method: Numerical effects, equation of state and boundary conditions, *Frontiers of Physics* 7 (2012) 481–490. doi:10.1007/s11467-012-0245-0.
- [70] Y. Gan, A. Xu, G. Zhang, Y. Li, H. Li, Phase separation in thermal systems: A lattice Boltzmann study and morphological characterization, *Physical Review E* 84 (2011) 046715. doi:10.1103/PhysRevE.84.046715.
- 275 [71] Y. Gan, A. Xu, G. Zhang, J. Wang, Y. Li, Y. Yang, Lattice Boltzmann kinetic modeling and simulation of thermal liquid-vapour system, *International Journal of Modern Physics C* 25 (2014) 1441002. doi:10.1141/S0129183114410022.

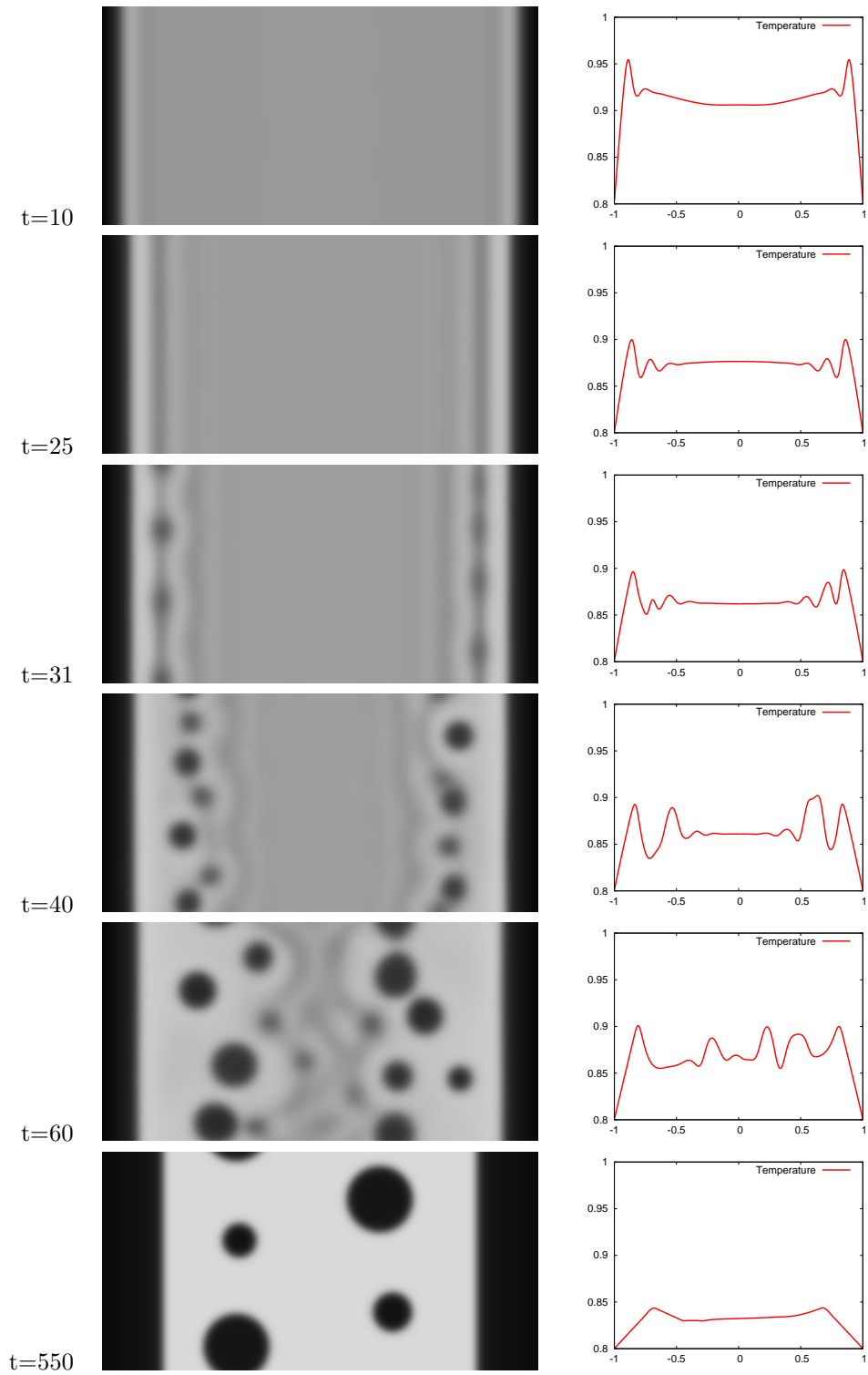


Figure 2: Snapshots of the phase separation between parallel walls (left column) and temperature profiles taken along the line $j = \mathfrak{N}_2/2$ (right column), at $t = 10, 25, 31, 40, 60$ and 550 (from top to bottom).

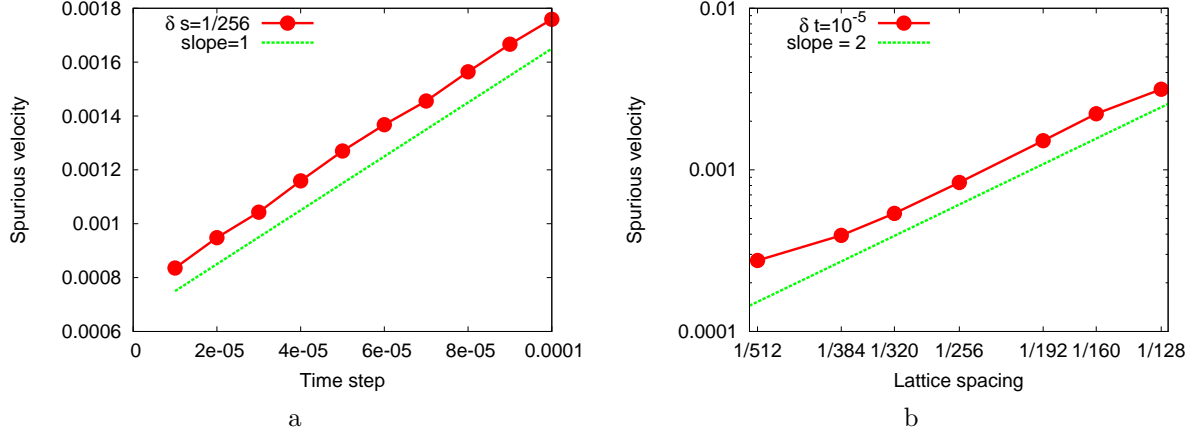


Figure 3: The dependence of the maximum value of the spurious velocity in the interface region vs: (a) the time step δt , for the lattice spacing $\delta s = 1/256$; (b) the lattice spacing δs , for the time step $\delta t = 10^{-5}$. The wall temperature is $T_w = 0.8$.

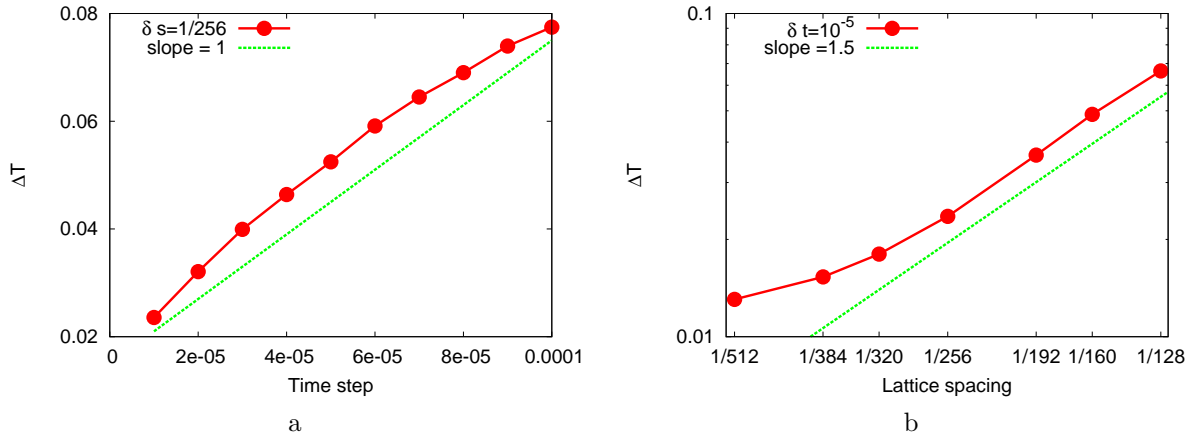


Figure 4: The dependence of the temperature difference $\Delta T = T_{max} - T_w$ between the maximum temperature T_{max} in the channel and the wall temperature T_w vs: (a) the time step δt , for the lattice spacing $\delta s = 1/256$; (b) the lattice spacing δs , for the time step $\delta t = 10^{-5}$. The wall temperature is $T_w = 0.8$.

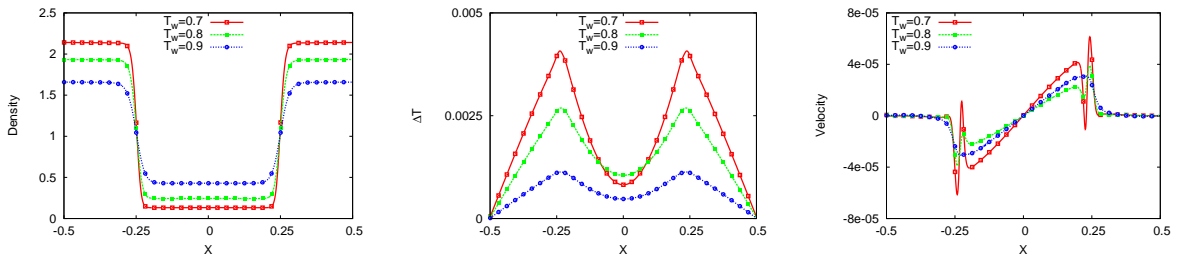


Figure 5: Profiles of the density $n(x)$, temperature difference $\Delta T(x) = T(x) - T_w$ and velocity component $u_x(x)$ in the steady state of the phase separation between parallel walls, for three values of the wall temperature $T_w = 0.7, 0.8, 0.9$. The time step and lattice spacing were set to $\delta t = 10^{-6}$ and $\delta s = 1/1024$.

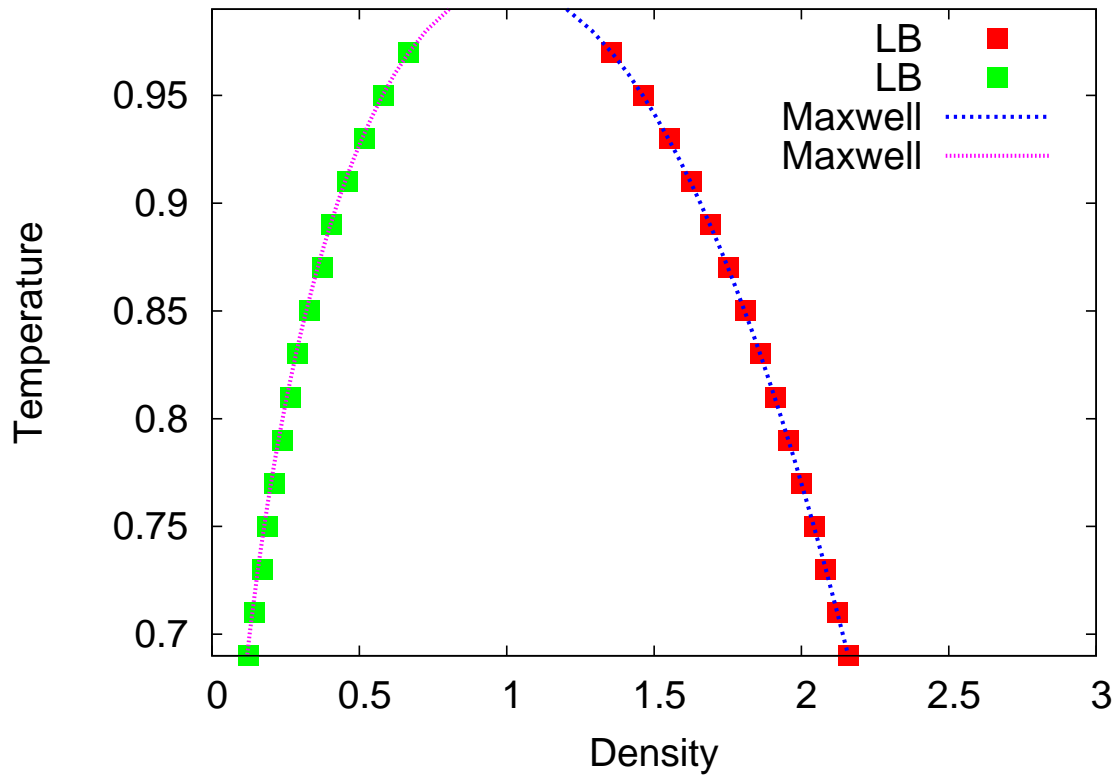


Figure 6: Phase diagrama of the fluid as compared with the Maxwell construction. The values $\delta s = 1/1024$ and $\delta t = 10^{-6}$ were used for this simulations.